HHS Public Access

Author manuscript

Nat Immunol. Author manuscript; available in PMC 2017 July 16.

Published in final edited form as:

Nat Immunol. 2017 March ; 18(3): 334–343. doi:10.1038/ni.3661.

Direct control of regulatory T cells by keratinocytes

Mariko Kashiwagi[1], **Junichi Hosoi**[1], **Jen-Feng Lai**[2], **Janice Brissette**[3], **Steven F. Ziegler**[2], **Bruce A. Morgan**[1], and **Katia Georgopoulos**[1]

[1]Cuteneous Biology Research Center, Massachusetts General Hospital, Harvard Medical School, Charlestown, MA, USA

[2]Immunology Program, Benaroya Research Institute at Virginia Mason, Seattle, WA, USA

[3]Department of Cell Biology, State University of New York Downstate Medical Center, Brooklyn, NY, USA

Abstract

Environmental challenges to epithelial cells trigger gene expression changes that elicit context-appropriate immune responses. Here we show that the chromatin remodeler Mi-2β controls epidermal homeostasis by regulating genes involved in keratinocyte and immune-cell activation to maintain an inactive state. Mi-2β depletion caused rapid deployment of both a pro-inflammatory and an immunosuppressive response in the skin. A key target of Mi-2β in keratinocytes was the pro-inflammatory cytokine thymic stromal lymphopoietin (TSLP). Loss of TSLP receptor (TSLPR) signaling specifically in regulatory T (T_{reg}) cells prevented their activation and permitted rapid progression from a skin pro-inflammatory response to a lethal systemic condition. Thus, in addition to their well-characterized role in pro-inflammatory responses, keratinocytes also directly support immune-suppressive responses that are critical for re-establishing organismal homeostasis.

Introduction

Skin integrity is maintained by the intimate interaction between epidermal keratinocytes and resident immune cells that supports recovery from a number of insults such as barrier disruption and bacterial or viral infection. Failure of the immune system to maintain

Correspondence should be addressed to M.K. (mariko.kashiwagi@cbrc2.mgh.harvard.edu) or K.G. (katia.georgopoulos@cbrc2.mgh.harvard.edu).

Accession codes

Gene Expression Omnibus: RNA-seq datasets have been deposited under the accession code GSE90573.

Author Contributions

M.K. designed and performed experiments and analyzed experimental data. J.H. designed and executed cytokine studies on primary cultured keratinocytes and advised on DC and DETC studies. J.F.L. provided experimental materials and advised on immunological studies. J.B. advised on keratinocyte transcriptional studies. S.F.Z. provided experimental materials and guidance throughout the project. K.G and B.A.M supervised research and analyzed data. M.K., K.G. and B.A.M wrote the manuscript.

Competing Financial Interests Statement

The authors declare no competing financial interests.

Data Availability Statement

Supporting data are available from M.K .and K.G.

tolerance or re-establish homeostasis after keratinocyte perturbation can cause autoimmune and chronic pro-inflammatory disorders that can give rise to skin neoplasias[1–3]. Despite considerable progress in keratinocyte and immune cell biology, the ways by which these distinct cell types communicate and coordinate with each other to maintain skin homeostasis remain ill-defined. Key to a productive interplay between keratinocytes and resident immune cells is an array of immune-regulatory factors that are either constitutively expressed or induced in keratinocytes or immune cells upon insult.

One of the cytokines that is rapidly induced in keratinocytes under stress is TSLP. TSLP is an IL-7-like epithelial cell-derived cytokine that signals through a hetero-dimeric receptor comprised of the TSLPR and the alpha subunit of the interleukin 7 receptor (IL-7Rα) that is expressed by many lymphoid, dendritic, myeloid and neuronal cell types[4,5]. Ectopic expression of TSLP in mouse skin has been correlated with a T helper type 2 (T_H2)-driven pro-inflammatory response in both skin and lung epithelia and an atopic dermatitis (AD)-like phenotype[4]. TSLP is highly expressed in both acute and chronic AD lesions in human patients but not in non-lesional skin from the same patient[4]. TSLP is thought to function by inducing expression of MHC class I and II and co-stimulatory molecules on dendritic cells (DCs), which can then promote the activation and differentiation of a naïve $CD4^+$ T cell into a pro-inflammatory T_H2 cell type[4]. Recent reports have shown that TSLP is also highly expressed in psoriatic lesions from human patients that have implicated a role in a T_H1 or T_H17 inflammatory response by promoting IL-23 production by DCs[6,7]. TSLP acts directly on $CD4^+$ and $CD8^+$ T cells to stimulate a pro-inflammatory response that can prevent development of skin epithelial tumors[8,9].

Mechanisms that control gene expression in keratinocytes are key to the keratinocyte's ability to respond to environmental insult and to elicit an immune response. Although signaling pathways and transcription factors are central mediators of stimulus-specific responses, chromatin regulators may also play a pivotal role in modulating transcription factor accessibility to appropriate regulatory sites upon receipt of a stress signal. Mi-2β is a nucleosome remodeler and a core component of the nucleosome remodeling deacetylase (NuRD) complex that is highly expressed in hematopoietic and epithelial tissues[10]. In the hematopoietic system, Mi-2β associates with the Ikaros family of DNA binding factors to control self-renewal and early lineage decisions through both positive and negative regulation of gene expression[11,12]. In the heart, the Mi-2β–NuRD complex is critical for maintaining cardiac muscle cell identity by repressing skeletal muscle-specific genes[13]. Mi-2β also regulates cell fate decisions at different stages of epidermal differentiation[14]. Ectodermal precursors rely on Mi-2β for establishing their self-renewing potential. However after establishment of self-renewal, epidermal precursors are not dependent on Mi-2β for maintenance but for specification into the follicular cell fate. These findings highlight a highly dynamic role for Mi-2β and the NuRD complex in the epidermal differentiation process, possibly by engaging with stage-specific transcriptional networks.

Here we examine the role of Mi-2β in keratinocytes of the adult skin and show that it is critical for maintaining skin homeostasis by repressing expression of genes normally induced in stressed keratinocytes. A key target of Mi-2β in basal keratinocytes is the gene encoding the cytokine sentinel of skin integrity, TSLP. We show that TSLPR was

specifically expressed in skin-associated T_{reg} cells and was required for inducing T_{reg} cell-suppressive functions under pro-inflammatory conditions. In this context, TSLP's role in mounting an immunosuppressive response supersedes its role as a pro-inflammatory factor in the skin. Our findings illustrate a heretofore unknown signaling mechanism, mediated by epithelial-derived regulatory signals, that plays an essential role in T_{reg} cell-dependent immune homeostasis in the skin.

Results

Mi-2β is critical for skin homeostasis

The role of the chromatin remodeler Mi-2β, encoded by the *Chd4/Mi-2b* gene, in the adult skin was investigated by inducing deletion in the basal epidermis. Two-month-old *Mi-2b*$^{loxF/loxF}$ *Krt14*-Cre-ERT2 (hereafter Mi2Δ) mice and littermate controls, lacking the *Krt14*-Cre-ERT2 transgene (hereafter wild-type), were injected with 4-hydroxytamoxifen (4-OHT) at days 0 and 3 and analyzed 7–30 days later. Depletion of Mi-2β protein in keratinocytes was mosaic at day 7 and nearly complete by day 9 (Fig. 1a–b). Potential depletion of Mi-2β in thymic epithelial cells, a subset of which expresses Keratin 14 (K14), was also tested using the 4-OHT injected *Krt14*-Cre-ERT2 *Rosa26*-yellow fluorescent protein (YFP) reporter mice. No YFP induction was seen in the thymus during the timeframe of our skin studies (data not shown).

At day 6–8 after initiation of Mi-2β deletion in the epidermis, mice developed a rough hair coat phenotype, indicative of a local skin inflammatory response. By day 9–11 mice exhibited flaky skin, weight loss and became progressively less active with a hunched posture, signs of progression from a local skin to a systemic response (Supplementary Fig. 1a). Nonetheless, by day 15 Mi-2Δ mice showed signs of remission, and by day 30 were fully recovered (Fig. 1c). Notably, at this later time point, Mi-2β-deficient keratinocytes were no longer detectable in the epidermis, which was comprised of wild-type keratinocytes (data not shown).

Histological examination of the skin at day 9 after Mi-2β depletion revealed hyperplasia in both the basal and suprabasal epidermal layers (acanthosis) with thickening of the cornified layer (Fig. 1d). Areas of moderate to severe hyperplasia were also seen in the follicular infundibulum but without hair follicle degeneration (Fig. 1d). A marked increase in the number of proliferating basal keratinocytes, normally minimal in adult skin, was observed (Fig. 1e, f). After a 2 h pulse-label with bromodeoxyuridine (BrdU), 42% of Mi-2β-depleted basal keratinocytes became BrdU positive compared to 1% in wild-type skin (Fig. 1f). K6, a marker of keratinocyte hyper-proliferation, was also detected early (day 7) after Mi-2β deletion at the suprabasal layer and only in cells deficient for Mi-2β, indicating a cell autonomous effect of the mutation (Fig. 1a). At later time points (day 9–11), K6 expression was seen throughout the epidermis, consistent with the widespread depletion of Mi-2β (Fig. 1g, K6). Mi-2β deficient basal keratinocytes were able to differentiate through the epidermal layers as indicated by an apparently normal distribution of layer-specific differentiation markers, such as K5, K1 and Loricrin in both wild-type and Mi2Δ skin (Fig. 1g). No barrier defect was observed, measured by an outward trans-epidermal water loss assay (data not shown). An increase in $CD45^+$ leukocytes and $CD4^+$ T cells in the dermis and in the

cellularity of skin-draining lymph nodes (sDLNs) was seen starting at day 7 of Mi2β depletion indicating a rapid immune response to genetically altered keratinocytes (Fig. 1h–i and Supplementary Fig. 1b).

Taken together, our data demonstrate that loss of Mi-2β in keratinocytes induces their activation and a pro-inflammatory response that progresses to a systemic condition. Nonetheless, upon displacement of the altered keratinocytes, full recovery and return to skin and organismal homeostasis is rapidly achieved.

Mi-2β represses pro-inflammatory genes in keratinocytes

The molecular basis of the epidermal phenotype manifested upon Mi-2β deletion was evaluated. Shortly after induction of Mi-2β deletion, basal keratinocytes were sorted and examined for changes in gene expression (day 7). Basal keratinocytes, expressing α_6 integrin (ITGA6) and lacking the CD34 and CD45 follicular stem cell and leukocyte markers were isolated from wild-type and Mi2Δ epidermis at the telogen phase of the hair cycle (Supplementary Fig. 2a). Gene ontology analysis of up-regulated genes in Mi2Δ relative to wild-type keratinocytes revealed induction of pathways supporting cell proliferation, keratinocyte activation and mobilization, normally activated by skin injury (Fig. 2a and Supplementary Fig. 2b)[15]. In addition, expression of genes encoding immune cell regulators, such as cytokines, chemokines and stress antigens was increased (Fig. 2a–b)[1].

Among the top five most highly induced genes in all categories was the epithelial cytokine *Tslp* (Fig. 2b). *Tgfb1,* involved in the differentiation of T_{reg} and T_H17 cells and in the migration of Langerhans cells (LCs), and *Bmp7* required for LC differentiation were also strongly induced (Fig. 2b)[16–18]. A modest increase in expression of cytokine genes *Il17d, Il1f9* (IL-36γ), *Il24, Kitl* and chemokine genes *Ccl22, Cxcl1*, *Cxcl9* and *Cxcl10* was detected (Fig. 2b)[1]. Genes encoding keratinocyte stress antigens that are engaged by receptors on dendritic epidermal γδ T cells (DETCs), including *Procr, Rae1 and Plxnb2* were up-regulated (Fig. 2b)[19–21]. *Cd74*, encoding a factor important for antigen presentation, and *Icam1*, encoding a cell adhesion molecule that mediates T cell recruitment to the skin, were also up-regulated (Fig. 2b)[22,23]. Finally, the antimicrobial and antiviral protein genes, *Lcn2, Oas3, Oasl1, Oasl2* were induced (Fig. 2b)[24].

TSLP expression in keratinocytes is normally induced in response to a variety of perturbations in skin structure or function[25–30]. Several lines of evidence suggested that induction of TSLP was a direct consequence of Mi-2β depletion. First, during the initial phase of Mi-2β deletion, immunohistochemistry confirmed early and cell autonomous induction of TSLP only in Mi2Δ keratinocytes in mosaically-deleted skin (Fig. 2c). Second, TSLP was induced in cultured keratinocytes after deletion of Mi-2β in *vitro,* eliminating the possibility of an indirect effect by an undetected barrier perturbation. 48 h after 4-OHT addition, induction of *Tslp* mRNA and secretion of TSLP protein were readily observed (Fig. 2d–e). As cultured keratinocytes prior to induction of *Mi-2b* deletion were proliferating, induction of TSLP mRNA upon *Mi-2b* deletion was not secondary to a keratinocyte proliferative response. Finally, the direct regulation of *Tslp* by Mi-2β was confirmed by Mi-2β chromatin immunoprecipitation combined with quantitative PCR.

Mi-2β enrichment was detected at previously characterized *Tslp* enhancer elements that are controlled by Nuclear factor-κB (NF-κB) (−3.9kb) and the Retinoid X receptor/Vitamin D receptor (VDR) complex (−4.2kb) respectively (Fig. 2f) [26,31]. In contrast to these enhancer sites, no enrichment was detected at the *Tslp* promoter (−0.3kb) or at intron 3 (Fig. 2f).

Thus the chromatin remodeler Mi-2β appears to be a key regulator of skin homeostasis by repressing expression of genes that support both activation and mobilization of keratinocytes and their immune cell neighbors. These genes are normally induced by transcriptional mechanisms responding to environmental inputs, but under homeostatic conditions are actively repressed by the Mi-2β–NuRD complex (Supplementary Fig. 2c).

TSLP-dependent protection of skin and organismal homeostasis

Induction of TSLP protein was readily seen in the Mi-2β-depleted epidermis and was likely associated with the rapid development of a pro-inflammatory condition. In an attempt to correct this phenotype, we crossed the constitutive *Crlf2* (TSLPR) null allele to the inducible *Mi-2b*$^{loxF/loxF}$ *Krt14*-Cre-ERT2 allele (*Crlf2*$^{-/-}$ *Mi-2b*$^{loxF/loxF}$ *Krt14*-Cre-ERT2, hereafter TMKO). Unexpectedly, a major fraction of the TMKO mice lost weight even faster than the Mi2Δ mice, became lethargic and died around day 10. In contrast, mice with Mi-2β skin deletion and lacking all lymphocytes showed a similar disease onset and recovery as seen in Mi2Δ mice (Fig. 3a, *Rag1*$^{-/-}$ *Mi-2b*$^{loxF/loxF}$ *Krt14*-Cre-ERT2, hereafter RMKO). A skin pro-inflammatory phenotype demarcated by expansion of the epidermal layers was also seen in RMKO mice by day 9, but was milder than that observed in Mi2Δ mice (Supplementary Fig. 3). An extensive expansion in a variety of myeloid cells including LCs and DCs was seen in RMKO compared to other mice (Supplementary Fig. 4). However, the systemic response and rapid demise was only seen in TMKO mice, indicating that this phenotype is lymphocyte-dependent (Fig. 3a).

We further evaluated the type of pro-inflammatory response induced by Mi-2β depletion and the effect of TSLPR signaling in this process. Expression of genes encoding pro-inflammatory cytokines was determined in skin biopsies. An increase in expression of genes encoding *Il2* and the T_H1- and T_H17-related cytokines, *Il1a, Il1b, Il6, Il18, Il23a*, *Tnf*, *Ifng* was detected in both Mi2Δ and TMKO skin, whereas the T_H2 cytokine encoding gene *Il4* was only up-regulated in Mi2Δ-mice. This result is consistent with a previously reported role of TSLP in supporting a T_H2 response. Among the commonly up-regulated cytokine genes, *Il2, Il1a, Il18* and *Ifng* were further induced in TMKO compared to Mi2Δ mice (Fig. 3b).

Phenotypic changes in epidermal keratinocytes and resident immune cells were also examined. Induction of keratinocyte activation and pro-inflammatory factors, such as K6, the Ki67 antigen and TSLP was seen in mice with Mi-2β depleted keratinocytes in the absence of TSLPR signaling (TMKO) or lymphocytes (RMKO) (Fig. 3c and Supplementary Fig.3a). Loss of dendrites and acquisition of a round morphology, hallmarks of DETC activation by keratinocyte stress antigens induced in Mi2Δ keratinocytes, were also seen independently of TSLPR signaling (Supplementary Fig.3b, Mi2Δ, TMKO). Similarly, activation and migration of skin LCs and DCs to sDLN upon Mi-2β deletion in keratinocytes, was independent of TSLPR signaling or the presence of lymphocytes (Supplementary Fig.4, Mi2Δ, TMKO and RMKO).

Taken together our studies indicate that *Tslp*, a major direct target of Mi-2β repression in keratinocytes, contributes but is not solely responsible for the skin pro-inflammatory response that rapidly develops in Mi2Δ mice. However, TSLPR signaling is required to prevent progression from a skin pro-inflammatory response to a lethal systemic condition.

Activation of skin T_{reg} cells is dependent on TSLP

We further evaluated the role of TSLPR signaling in skin-associated T cells under homeostatic and pro-inflammatory conditions (Mi2Δ). An increase in sDLN cellularity and in the absolute number of $CD4^+$ and $CD8^+$ T cells was seen in both Mi2Δ and TMKO relative to wild-type mice (Fig. 4a and Supplementary Fig. 5a). These cell numbers were modestly reduced in TMKO compared to Mi2Δ, supporting TSLP's contribution to Mi2Δ skin inflammatory response but also highlighting that TSLP is not the only contributing factor in this mouse pro-inflammatory model.

A profound increase in immunosuppressive $CD4^+Foxp3^+$ T_{reg} cells, was seen in sDLNs from early time points of Mi2Δ deletion (Fig. 4a–b)[32–34]. T_{reg} cells from Mi2Δ sDLNs displayed an activated effector cell phenotype with higher expression of CD25, CD44, CTLA4, CD103, KLRG1 TNFR2 and the Ki67 antigen (Fig. 4b and Supplementary Fig. 5b)[35–37]. Furthermore, T_{reg} cells associated with Mi2Δ pro-inflammatory skin had a strong *in vitro* immunosuppressive activity compared to normal skin-associated T_{reg} cells (Fig. 4c and Supplementary Fig. 5c). However, in the absence of TSLPR signaling, T_{reg} cell numbers were very modestly increased especially compared to wild-type T_{reg} cells from Mi2Δ skin (Fig. 4a,d, ~3 fold reduction in TMKO compared to Mi2Δ). In addition, expression of activation receptors, co-inhibitory molecules, memory and effector markers, were lower in TSLPRΔ T_{reg} cells compared to wild-type T_{reg} cells from Mi2Δ sDLNs (Fig. 4b and Supplementary Fig. 5b).

In contrast to the significant reduction in T_{reg} cells, $CD4^+Foxp3^-$ effector T cells (T_{eff} cells) were less affected by the loss in TSLPR with a small reduction in numbers seen in TMKO compared to Mi2Δ (Fig. 4a,d, ~1.2 fold reduction). T_{eff} cells from both mutants displayed an activated effector cell phenotype with increased expression of CD44 and CD69 (Supplementary Fig. 5b), and upon *in vitro* re-stimulation expressed higher amounts of TNF, IL-2 and IFN-γ compared to their wild-type sDLN counterparts (Supplementary Fig. 5d). Protein expression of IL-4, IL-13 or IL-17A were not readily detected in the $CD4^+$ T cell re-stimulation assay with cells from either TMKO or Mi2Δ mice (data not shown).

In summary, our data shows that whereas the role of TSLP as a skin pro-inflammatory factor can be redundant, its apparent role as an immune-suppressive factor is not. Importantly, TSLPR signaling correlates with the rapid activation of skin T_{reg} cells and potent immunosuppressive function.

Direct regulation of skin T_{reg} cells by TSLP

A potential direct role of TSLPR in the functional activation of skin-associated T_{reg} cells was further evaluated. T_{reg} cells isolated from the skin and sDLNs expressed more TSLPR compared to other $CD4^+$ T cells present at these sites (Fig. 5a). Nonetheless, the increase in TSLPR expression in T_{reg} cells compared to other $CD4^+$ T cells was diminished in the

spleen (Fig. 5a). These data suggest that skin-associated T_{reg} cells are specifically conditioned to respond to TSLP, normally induced by keratinocyte perturbation, by higher expression of the TSLP signaling receptor.

The direct role of TSLPR signaling in T_{reg} cell function was tested in adoptive transfer studies. Wild-type and Mi2Δ mice, bearing the *Foxp3*-IRES-EGFP knock-in alleles, were lethally irradiated and used as recipients for bone marrow from mice with conditional deletion of TSLPR in T_{reg} cells (*Foxp3*-IRES-Cre *Crlf2*$^{loxF/loxF}$, hereafter TSLPRΔ T_{reg} cell). 8–12 weeks after transplantation, both wild-type and Mi2Δ chimeras were treated with 4-OHT and harvested 8–11 days later. Foxp3$^+$ T_{reg} cells were subdivided into TSLPRΔ donor and TSLPR wild-type recipient based on EGFP expression (Supplementary Fig. 6a–b). Under homeostatic conditions the ratio of TSLPRΔ donor to wild-type recipient cells was ~ 2:1 in wild-type skin and sDLN (Supplementary Fig. 6c. WT). However, upon skin depletion of Mi-2β, the ratio was reduced to 0.7:1 (Supplementary Fig. 6c, Mi2Δ), reflecting a preferential expansion of TSLPR wild-type recipient relative to the TSLPRΔ donor T_{reg} cells (Supplementary Fig. 6b–c). The Mi2Δ bone marrow chimeras with TSLPRΔ T_{reg} cells developed disease scores similar to those seen in Mi2Δ mice possibly due to expansion of the endogenous radio-resistant TSLPR wild-type T_{reg} cells that provided immunosuppression and protection against development of a lethal systemic response.

To further evaluate the functionality of T_{reg} cells expanded in the skin by cell autonomous TSLPR signaling, a second adoptive transfer model was generated. Rag or RMKO mice were sub-lethally irradiated and reconstituted with bone marrow from mice with TSLPRΔ T_{reg} cells. Bone marrow from mice with intact TSLPR signaling in T_{reg} cells (*Foxp3*-IRES-Cre *Crlf2*$^{loxF/+}$, hereafter TSLPR$^+$ T_{reg} cell) was used as a control. 8–12 weeks after transplantation, both Rag and RMKO chimeras were treated with 4-OHT. By day 7 after Mi-2β deletion, RMKO mice reconstituted with TSLPRΔ T_{reg} cells but with an otherwise TSLPR-competent immune system developed a severe disease phenotype (Fig. 5b, RMKO:TSLPRΔ T_{reg}). This result was in contrast to RMKO mice that received TSLPR$^+$ T_{reg} cells (Fig. 5b, RMKO: TSLPR$^+$ T_{reg}). Both the severity and time frame of the disease in RMKO: TSLPRΔ T_{reg} chimeras and the milder disease phenotype seen in RMKO: TSLPR$^+$ T_{reg} chimeras were similar to those previously seen in TMKO or in Mi2Δ mice. Thus under skin pro-inflammatory conditions, TSLPR signaling in T_{reg} cells prevents progression to a severe systemic response.

Consistent with an impairment in T_{reg} cell function, the sDLN cellularity was greater in RMKO:TSLPRΔ T_{reg} chimeras compared to RMKO: TSLPR$^+$ T_{reg} chimeras (Fig. 5c). A greater expansion of T_{eff} cells was also seen in both the skin and sDLNs of RMKO:TSLPRΔ T_{reg} chimeras (Fig. 5d–g, T_{eff} and Supplementary Fig. 7a). Although the number of skin-associated T_{reg} cells with or without TSLPR signaling was similar in the two types of RMKO chimeras, possibly due to the short time of allowed analysis after Mi-2β deletion (Fig. 5d–g, T_{reg} and Supplementary Fig. 7a), induction of activation markers, such as CTLA4, CD103 and CD25, was consistently reduced in the absence of TSLPR signaling in these cells as in the TMKO mice (Fig. 5h and Supplementary Fig. 7b). Thus under skin pro-inflammatory conditions, TSLPR signaling in skin T_{reg} cells was required for their activation and ability to repress expansion of local effector T cells.

We also tested the role of IL-2R signaling in Mi2Δ skin T_{reg} cells. Treatment of mice with an antibody to IL-2Rα (anti-CD25) has been shown to cause a transient reduction in T_{reg} cells[38]. After anti-CD25 treatment a severe reduction in T_{reg} cells was observed in normal skin under homeostatic conditions compared to untreated controls (Supplementary Fig. 8, WT:PBS vs. WT:αCD25). However, after Mi-2β deletion in the skin (days 8–14), the number of skin T_{reg} cells was increased whether the mice were previously treated with anti-CD25 or not (Supplementary Fig. 8, Mi2Δ:PBS vs. Mi2Δ:αCD25). At both early and later time points of Mi-2β deletion an expansion of skin T_{reg} cells was seen in spite of the anti-CD25 treatment. Thus although IL-2 is critical for T_{reg} cell maintenance under skin homeostatic conditions, under skin pro-inflammatory conditions TSLP secreted by activated keratinocytes can drive T_{reg} cell expansion.

In summary, skin T_{reg} cells are conditioned to respond to changes in their local environment by expressing TSLPR. Early induction of TSLPR signaling in skin T_{reg} cells, is critical for balancing local immune cell responses and preventing their uncontrolled dissemination to the periphery.

TSLPR signaling augments T_{reg} effector transcription

We next examined the global effect of TSLPR signaling on the expression of genes responsible for T_{reg} cell effector function. Wild-type or TSLPRΔ T_{reg} cells were isolated from sDLN associated with Mi-2β depleted pro-inflammatory skin (WT T_{reg}: Mi2Δ and TSLPRΔ T_{reg}: Mi2Δ) and used for RNAseq studies. Wild-type T_{reg} cells from sDLN associated with homeostatic skin were used as controls (WT T_{reg}: Hom). Differential gene expression analysis of wild-type T_{reg} cells from pro-inflammatory compared to homeostatic skin has shown that 1321 genes were up-regulated and 925 genes were down-regulated (Fig. 6a, Supplementary Table 1–2). A similar trend of up- and down-regulated genes was seen with TSLPRΔ T_{reg} cells from pro-inflammatory skin (Fig. 6a, TSLPRΔ T_{reg}: Mi2Δ vs. WT T_{reg}: Mi2Δ). However, the changes in gene expression detected in TSLPRΔ T_{reg} cells never reached the level detected in wild-type T_{reg} cells under similar pro-inflammatory conditions (Fig. 6a–c).

Genes encoding transcription factors required for the transition of naive T_{reg} cells to an activated effector state, such as *Irf4 and Prdm1* (Blimp1) and those important in T_H17 cells such as *Ahr, Rora, Ikzf3* were up-regulated in wild-type T_{reg} cells under skin pro-inflammatory conditions compared to homeostatic conditions (Fig. 6d) [39–41]. Genes involved in migration and epithelial localization of T_{reg} cells such as *Ccr4, Ccr8, Ccr10* and *Fut7* were also strongly induced whereas *Ccr7* was reduced in activated compared to resting wild-type Treg cells (Fig. 6d)[35,36,42,43]. Genes involved in T_{reg} cell-mediated immunosuppression such as the co-stimulatory molecule *Icos,* the co-inhibitory molecules *Ctla4, Lgals1*(Galectin1), *Tigit* and *Havcr2* (Tim3), the cytotoxic molecule *Gzmb* (Granzyme B), effector molecules *Fgl2* (Fibrinogen-like protein 2) and *Ebi3* (component of IL-35) were also strongly up-regulated (Fig. 6d)[44,45]. The immunosuppressive cytokine *Il10* was not markedly expressed in either activated or resting T_{reg} cells (Fig. 6d). Notably, induction of these genes involved in the immunosuppressive response was greatly compromised in TSLPRΔ T_{reg} cells (Fig. 6d).

In summary, TSLPR signaling is a major contributor to the expression of genes that support a T_{reg} cell's immune-suppressive function in the context of a pro-inflammatory skin response (Supplementary Fig. 9). Many of these genes are induced in the absence of TSLPR signaling, however overall their expression is insufficient to support T_{reg} cell suppressor function.

Discussion

In its function as the barrier between the body and the outside world, the skin must respond to pathogenic insult by rapidly initiating a repair response and by deploying a pro-inflammatory reaction. The work reported here reveals that the chromatin remodeler Mi-2β in the NuRD complex holds these two components of a skin response poised for rapid deployment upon injury. The first component includes growth factors and structural proteins that comprise an autocrine repair mechanism that is normally induced by wounding. The second component includes a panoply of stress-induced antigens, anti-microbial proteins, cytokines and chemokines that selectively target activation and mobilization of skin resident immune cells in response to environmental insults. Loss of Mi-2β in basal keratinocytes was demarcated by hyperplasia in both the basal and suprabasal epidermal layers with thickening of the cornified layer and rapid development of an inflammatory response.

Of the pro-inflammatory cytokines induced in Mi-2β deficient keratinocytes, TSLP was the most prevalent. The *Tslp* gene was directly repressed by Mi-2β binding to an enhancer region also regulated by the VDR and NF-κB. TSLP is a known sentinel of epithelial cell barrier integrity that can promote T_H2 cytokine-mediated skin inflammation. In agreement with previous studies, in the absence of TSLPR signaling, the T_H2 response was diminished in the Mi-2β deficient skin. However, T_H1 and T_H17 responses were largely unaffected and possibly increased. Activation of skin resident immune populations such as DETCs and DCs was also seen regardless of TSLPR signaling. These findings indicate that although TSLPR signaling contributes to a skin pro-inflammatory response initiated by loss of Mi-2β, this pro-inflammatory activity is redundant with other signals.

In contrast, an unexpected and non-redundant role of TSLPR signaling in resolving an inflammatory response was revealed in these experiments. A rapid increase in T_{reg} cells with an effector phenotype and strong *in vitro* immunosuppressive properties was seen in M-2βΔ skin and sDLNs. TCR ligation is not normally sufficient to activate T_{reg} cells and an additional signal provided by the environment in the form of a cytokine such as IL-2 is required for full T_{reg} cells suppressive activity in situ. Unexpectedly, TSLP a pro-inflammatory cytokine secreted by M-2β deficient keratinocytes was critical for the activation of skin T_{reg} cells. In principle, TSLPR signaling could activate skin T_{reg} cells either directly or indirectly by acting through another immune cell such as a DC. Using bone marrow chimeras generated by reconstituting lymphocyte-deficient mice with an immune system in which TSLPR signaling was defective only in T_{reg} cells, we demonstrated that TSLPR signaling was directly required in skin T_{reg} cells to promote their activation, to control expansion of local T_{eff} cells and protect against development of a lethal systemic response.

T_{reg} cells from Mi-2β depleted skin showed a highly activated effector phenotype that was underscored by increase in expression of transcription factors such as *Irf4* and *Prdm1*, co-inhibitory and effector molecules *Ctla4*, *Tigit, Lgals1, Fgl2* and *Gzmb*, and chemokine receptors such as *Ccr4, Ccr8* and *Ccr10.* Induction of these factors, critical for Treg cell function, was impaired by loss in TSLPR signaling. It is noteworthy that TSLP also induces expression of the CCR4 ligands, CCL17 and CCL22 in DCs, thereby affecting the migration of activated skin Tregs by influencing two independent cell types[46]. The transcriptional profile of Mi2Δ skin-associated T_{reg} cells complemented the transcriptional profile of Mi-2β depleted keratinocytes that express many T_H1 and T_H17 promoting cytokines and the T_H1 phenotype of CD4 T cells associated with Mi-2β depleted sDLN. Both T cell and DC inhibitory factors were strongly up-regulated in these skin effector T_{reg} cells raising the possibility that lack of proper induction upon loss of TSLPR signaling may allow aberrant activation of DCs and effector T cells that is rapidly disseminated in the periphery.

STAT5 was recently reported to be critical for the suppressive function of T_{reg} cells[47]. STAT5 is activated in response to IL-2R signaling in T_{reg} cells and its activation is sufficient to rescue their function in the absence of IL-2R. In this context, it is noteworthy that TSLPR signaling activates STAT5 in other cell types and also contributes to STAT5 activation in T_{reg} cells[48–50]. We also found that anti-CD25 treatments that are sufficient to deplete T_{reg} cells in normal skin did not prevent activation of T_{reg} cells upon Mi-2β deletion in keratinocytes *in vivo*. We thus propose that the TSLP-TSLPR-STAT5 cascade rapidly induces the transcriptional changes that support an activated T_{reg} cell phenotype required at the initial phase of a skin pro-inflammatory response. At a later phase of the response increased production of IL-2 by other immune cells may sustain T_{reg} cell activation. However, the initial rapid induction of skin T_{reg} cells by TSLP is critical for controlling the aberrant spread of a local response and preventing loss of organismal homeostasis.

Our studies provide new insights into the epigenetic factors that regulate skin repair and damage control pathways in keratinocytes and an unexpected role of pro-inflammatory cytokines, such as TSLP, in immune-suppression. The direct role of TSLP in inducing highly immunosuppressive T_{reg} cells tailored to the needs of their local environment has important consequences for organismal health. Insight from our mouse model may inform the management of inflammatory skin diseases, in which the prevalent paradigms are based on TSLP's pro-inflammatory action.

Online Methods

Mice

Mi-2b$^{loxF/loxF}$ mice were generated in the Georgopoulos lab[12]. *Crlf2*(TSLPR)$^{-/-}$ and *Foxp3*-IRES-Cre *Crlf2*$^{loxF/loxF}$ mice were generated in the Ziegler lab[51,52]. *Krt14*-CreERT2 transgenic and *Foxp3*-IRES-EGFP knockin (KI) mice were obtained from P. Chambon and V.K. Kuchroo respectively[53,54]. *Rag1*$^{-/-}$ mice were purchased from Jackson laboratories. All strains of mice used in this study were on the C57BL/6 background. *Mi-2b*$^{loxF/loxF}$*Krt14*-CreERT2 (Mi2Δ) were crossed with *Crlf2*$^{-/-}$ or *Rag1*$^{-/-}$ to generate *Crlf2*$^{-/-}$ *Mi-2b*$^{loxF/loxF}$*Krt14*-CreERT2 (TMKO) or *Rag1*$^{-/-}$*Mi-2b*$^{loxF/loxF}$*Krt14*-CreERT2 (RMKO) mice. Mi2Δ and TMKO mice were crossed with *Foxp3*-IRES-EGFP *KI* mice to facilitate

studies with $CD4^+$ T_{reg} cells in these mutant mice. All mice were bred and maintained in pathogen-free conditions in the animal facility at Massachusetts General Hospital. At the time of analysis, mice were 2–3 months of age. All animal experiments were done according to protocols approved by the Subcommittee on Research Animal Care at Massachusetts General Hospital (Charlestown, Massachusetts) and in accordance with the guidelines set forth by the US National Institutes of Health. Gene inactivation was achieved by intraperitoneal (i.p.) injection of mice with 0.5 mg of 4-OHT (Sigma-Aldrich) delivered twice with a three-day interval. Mice were monitored for clinical symptoms and staged from 0–4, as follows: 0, no clinical expression of disease; 1, rough hair coat on the ventral side; 1.5, rough hair coat on both sides; 2, loss of weight; 2.5, less movement; 3, hunched; 3.5, no movement, very thin; 4, dead. Mice that were close to disease stage 3.5 were sacrificed and excluded from any further phenotypic analysis of immune cell populations.

Histology and Immunofluorescence

Dorsal skins were frozen in OCT, sectioned at 6 μm and used for Hematoxylin and Eosin staining or for immunofluorescence. Sections were fixed in 4% formaldehyde and subjected to indirect immunofluorescence. When staining with mouse mAbs, the MOM Fluorescent Kit (Vector) was used. Primary antibodies used were: mouse monoclonal Mi-2β [16G4][10], rabbit polyclonal K5 (BAbCo), rabbit polyclonal K1 (BAbCo), rabbit polyclonal Loricrin (BAbCo), rabbit polyclonal K6 (BAbCo), goat polyclonal TSLP (R&D), rat monoclonal Ki67 (BD Biosciences, SolA15). Fluorescence-conjugated secondary antibodies for primary antibodies developed in rabbit, rat, or goat were obtained from Jackson ImmunoResearch Laboratories. For BrdU incorporation analysis, mice were injected i.p. with BrdU (100 μg/g body weight) (Molecular Probes). 2 h later, dorsal skin was harvested and stained with BrdU-specific antibody conjugated with Alexa Fluor 546 (Molecular Probes). DAPI was used to stain nuclei. Images were taken with the Olympus BX50 or Nikon A1 Confocal microscope.

Preparation of single cell suspension from ear skin and dorsal skin

Ear or dorsal skins were cut in pieces, and incubated for 20–30 min at 37 °C in RPMI containing 5% FCS, collagenase D (Roche) or Liberase TM (Roche) and DNase I. Cells were then washed three times in ice-cold RPMI containing 10% FCS and 2 mM EDTA.

Flow cytometry of immune cell populations

Phenotypic analysis of cells from skin or sDLNs was performed by flow cytometry using a FACSCanto (BD Biosciences). Data was analyzed with the FlowJo software (Tristar). The antibodies used were CD45 (30-F11), CD3ε (2C11), MHC class II (M5/114), CD11c (HL3), CD207 (4C7), EpCAM (G8.8), CD80 (16-10A1), CD86 (GL1), CD40 (1C10), TCRβ (H57-597), TCRγδ (GL3), CD8 (53-6.7), CD4 (GK1.5 or RM4), Foxp3 (FJK-16s), CD25 (PC61), CD44 (IM7), CD69 (H1.2F3), IL2 (JES6-5H4), TNF (MP6-XT22), IFN-γ (XMG1.2), IL-4 (11B11), IL-13 (eBio13A), IL-17A (eBio17B7), Ki67 (SolA15), CTLA4 (UC10-4B9), CD103 (2E7), KLRG1 (2F1), TNFR2 (TR75-89), TSLPR (produced by the Ziegler lab)[49].

Isolation of basal keratinocytes from dorsal epidermis

Dorsal epidermis was separated from the dermis after overnight digestion at 4 °C in 0.25% trypsin. The epidermis was washed three times in PBS and stirred for 10 min in PBS containing 10% Ca^{2+}-depleted fetal calf serum (FCS). Cells were then stained with anti-CD45 (30-F11), anti-CD34 (RAM34), and anti-ITGA6 (eBioGoH3) and basal keratinocytes were sorted as $ITGA6^{+}CD34^{-}CD45^{-}$ using a MoFlo sorter (Cytomation). Two independent sorts of basal keratinocytes from wild-type N=3 and Mi2Δ N=2 mice were used for two RNA-seq experiments.

RNA-sequencing, gene-expression and pathway analysis

Total RNA was isolated with RNeasy kit (QIAGEN). NEXTflex RNAseq kit (BIOO scientific) or a Trueseq stranded mRNA sample prep kit (Illumina) were used for construction of cDNA libraries for RNA-Sequencing. The cDNA libraries were ligated with indexed primers, followed by 15 cycles of PCR amplification. The amplified libraries were multiplexed and sequenced by Illumina Hiseq2000 at the Bauer Center of Harvard University. Raw sequencing files were subjected to quality control using FastQC. Read alignment was performed on the mm9 or mm10 assembly of the mouse genome using either the Burrows-Wheeler or the STAR genome alignment algorithms[55,56]. Read normalization and differential gene expression was performed with the Deseq2 algorithm through HOMER implementation of the R platform[57,58]. Heat maps of normalized exon read counts for differentially expressed genes were generated with Cluster 3.0 (open source software developed by Michael Eisen) and visualized with Java TreeView (open source software developed by Alok J. Saldanha). Differentially expressed genes shown in the heatmap of Fig. 6a were filtered for having a value of 64 normalized raw reads in at least one sample and a difference of 1 between the maximum and minimum log2 transformed normalized raw reads. DAVID Bioinformatics Resources 6.7 was used for Gene Ontology analysis[59]. Changes in gene expression as determined by cumulative distribution function plot was also analyzed by the Kolmogorov-Smirnov test (GraphPad Prism). $P<0.05$ was considered significant. The RNA-seq datasets were deposited to the GEO series database (GSE90573).

Induction of Mi-2β deletion in primary cultured keratinocytes

Cultures were prepared from newborn *Mi-2b*$^{loxF/loxF}$ *Krt14*-CreERT2 mice and grown to confluence in low-calcium keratinocyte growth medium (GIBCO) at 37 °C, 5% CO_2. After reaching 80% confluence, cells were treated with 300 nM 4-OHT in DMSO for 16 h at 37 °C, 5% CO_2. Cells were then washed three times with PBS, fresh media were added and cells were incubated for 32 h prior to RNA preparation or for 56 h prior to collection of conditioned media.

RT-qPCR

Total RNA was extracted with Trizol (Invitrogen) and purified with RNeasy kit (QIAGEN), followed by reverse transcription with the Superscript III RT-PCR system (invirogen). qPCR analyses were performed on 7000 real-time PCR system (Applied BioSystems) using gene-specific primer pairs. Data were normalized by the abundance of the *Actb* transcript. The sequences of primers are listed in Supplementary Table 3.

Antibody array

Secretion of TSLP in conditioned media was measured by the Mouse Cytokine Antibody Array 4 (RayBio) according to the manufacturer's protocol.

ChIP-qPCR

Mi-2β ChIP was performed as described previously[60]. Briefly, chromatin was prepared from primary cultured keratinocytes from newborn wild-type mice, followed by ChIP with anti-Mi-2β (16G4, 2G8, 17H11 and 16F5; produced in house). ChIPed DNA was subjected to analysis by real-time qPCR. Fold enrichment was calculated as [target/negative control (intergenic region of Chr5)] for anti-Mi-2β ChIP/[target/negative control] for the input. The sequences of primers are listed in Supplementary Table 3.

Preparation of epidermal sheets and Immunofluorescence

The epidermal sheet of ear skin was separated from the dermal layer by digestion at 37 °C in 0.25% trypsin for 10 min. The epidermis was washed three times in PBS, fixed for 15 min at −20 °C in ice-cold acetone, washed two times in PBS, and rehydrated for 30 min at 25 °C in PBS. Nonspecific binding on the epidermis was then blocked with two incubations in 1% BSA and 0.1% Tween-20 in PBS, followed by overnight incubation at 4 °C with FITC-conjugated anti-CD3ε (2C11) or anti-CD207 (4C7), followed by TRITC-conjugated secondary antibodies.

Purification of CD4$^+$ T cell subsets

CD4$^+$Foxp3-GFP$^-$ T_{eff} cells, CD4$^+$CD62L$^+$Foxp3-GFP$^-$ naïve T cells and CD4$^+$Foxp3-GFP$^+$ T_{reg} cells were isolated from sDLNs (axillary, brachial, and inguinal) or spleen after depletion of CD8$^+$ T cells (anti-CD8α), B cells (anti-IgM), myeloid cells (anti-CD11b) and erythroid cells (anti-Ter119) using magnetic beads conjugated to BioMag goat anti-rat IgG (QIAGEN). Cells remaining after depletion were labeled with fluorochrome-conjugated anti-CD4, CD62L and CD25 for phenotypic analysis. CD4$^+$Foxp3-GFP$^-$, CD4$^+$CD62L$^+$Foxp3-GFP$^-$ or CD4$^+$Foxp3-GFP$^+$ cells were sorted using a MoFlo sorter (Cytomation). Sorted cells were subjected to *in vitro* culture or RNA-seq studies. RNA-seq experiments were performed with two independent sorts of T_{reg} cells each from sDLNs of wild-type N=7 and Mi2Δ N=2 mice and one sort of T_{reg} cells from sDLNs of TMKO N=6 mice.

In vitro T_{reg} cell suppression assay

Sorted CD4$^+$Foxp3-GFP$^+$ T_{reg} cells were co-cultured with sorted CD4$^+$CD62L$^+$Foxp3-GFP$^-$ naïve T cells that were stimulated with anti-CD3ε ε (1 μg/ml) in the presence of irradiated antigen presenting cells (APCs) for 3 days at 37 °C, 5% CO_2. APCs, isolated from wild-type spleens after T cell depletion using anti-CD4 and anti-CD8 magnetic beads (Miltenyi Biotec), or *Rag1*$^{-/-}$ spleens were irradiated prior to use.

In vitro re-stimulation of CD4$^+$ effector T cells

Sorted CD4$^+$Foxp3-GFP$^-$ cells were cultured for 16 h in RPMI containing 10% FCS in the presence of anti-CD3ε (2 μg/ml) and anti-CD28 (1 μg/ml) at 37 °C, 5% CO_2. Cells were then re-stimulated with PMA plus ionomycin for 4 h in the presence of brefeldin A.

Cell-cycle analysis

Cells were fixed overnight at 4 °C in 70% ethanol. Fixed cells were stained for 30 min at 37 °C with propidium iodide staining buffer (250 μg/ml RNase A and 50 μg/ml propidium iodide (PI)), and DNA content was analyzed by FACSCanto and FlowJo software.

Generation of bone marrow chimeras

Bone marrow from *Foxp3*-IRES-Cre *Crlf2*$^{loxF/loxF}$ mice was used in adoptive transfers as a source of TSLPRΔ T_{reg} cells. Bone marrow from *Foxp3*-IRES-Cre *Crlf2*$^{loxF/+}$ mice with intact TSLR signaling in T_{reg} cells was used as a control. 4×10^6 bone marrow cells were transferred into lethally irradiated (500 rads twice, 16h apart) wild-type or Mi2Δ recipients or sub-lethally irradiated (300 rads twice, 16 h apart) RagΔ or RMKO recipients. 8–12 weeks after reconstitution Mi-2β deletion was induced with 4-OHT delivered twice within a three-day interval. WT and Mi2Δ chimeras were analyzed 8–11 days after 4-OHT administration. Rag and RMKO chimeras were analyzed at 7 days later.

In vivo IL-2Rα blockade

Mice were injected i.p. with 400 μg/mouse anti-CD25 (PC61) 5 days before inducing Mi-2β depletion with 4-OHT[38]. A PBS-injected group was used as a control.

Statistical analysis

A two-tailed unpaired t-test was used to calculate differences between two groups (GraphPad Prism). *P* values <0.05 were considered significant. The *F*-test was applied to determine variation within groups and Welch's correction to the t-test was applied to groups with unequal variances. Statistical tests were not used to pre-determine group size, samples were not randomized and investigators were not blinded to experimental group allocations.

Supplementary Material

Refer to Web version on PubMed Central for supplementary material.

Acknowledgments

This research was supported by NIH R21 AR055813, RO1 AR064390 and R01AR069132 to K.G., NIH RO1 AI068731 and PO1 HL098067 to S.F.Z. and NIH R01 AR055256 to B.A.M. K.G. is an MGH scholar supported by J. de Gunzburg. J.H was supported by a Shiseido grant. High-throughput RNA sequencing was performed at the Bauer Center for Genomic research Harvard University, Cambridge. We thank P. Chambon (Institute of Genetics and Cellular and Molecular Biology) and V.K. Kuchroo (Brigham and Women's Hospital) for the *Krt14*-CreERT2 mice and *Foxp3*-IRES-EGFP mice respectively. We thank M.E. Bigby for consultation on lymphocyte isolation from the skin and L.M. Francisco and A.H. Sharpe for consultation on T_{reg} cell and DC analysis. We thank E. Wu and B. Czyzewski for mouse husbandry, A. Cho, M. Ahl, J.E. King, and J. Brandollni for bone marrow transplantation and T. Minegishi for R platform support. We also thank JM. Park, H. Cantor, H.J. Kim, F. Gounari and K. Khashayarsha for critical comments on the manuscript.

References

1. Pasparakis M, Haase I, Nestle FO. Mechanisms regulating skin immunity and inflammation. Nat Rev Immunol. 2014; 14:289–301. [PubMed: 24722477]
2. Kupper TS, Fuhlbrigge RC. Immune surveillance in the skin: mechanisms and clinical consequences. Nat Rev Immunol. 2004; 4:211–222. [PubMed: 15039758]
3. Rangwala S, Tsai KY. Roles of the immune system in skin cancer. Br J Dermatol. 2011; 165:953–965. [PubMed: 21729024]
4. Liu YJ, et al. TSLP: an epithelial cell cytokine that regulates T cell differentiation by conditioning dendritic cell maturation. Annu Rev Immunol. 2007; 25:193–219. [PubMed: 17129180]
5. Wilson SR, et al. The epithelial cell-derived atopic dermatitis cytokine TSLP activates neurons to induce itch. Cell. 2013; 155:285–295. [PubMed: 24094650]
6. Volpe E, et al. Thymic stromal lymphopoietin links keratinocytes and dendritic cell-derived IL-23 in patients with psoriasis. J Allergy Clin Immunol. 2014; 134:373–381. [PubMed: 24910175]
7. Guttman-Yassky E, et al. Low expression of the IL-23/Th17 pathway in atopic dermatitis compared to psoriasis. J Immunol. 2008; 181:7420–7427. [PubMed: 18981165]
8. Demehri S, et al. Elevated epidermal thymic stromal lymphopoietin levels establish an antitumor environment in the skin. Cancer Cell. 2012; 22:494–505. [PubMed: 23079659]
9. Di Piazza M, Nowell CS, Koch U, Durham AD, Radtke F. Loss of cutaneous TSLP-dependent immune responses skews the balance of inflammation from tumor protective to tumor promoting. Cancer Cell. 2012; 22:479–493. [PubMed: 23079658]
10. Kim J, et al. Ikaros DNA-binding proteins direct formation of chromatin remodeling complexes in lymphocytes. Immunity. 1999; 10:345–355. [PubMed: 10204490]
11. Yoshida T, et al. The role of the chromatin remodeler Mi-2beta in hematopoietic stem cell self-renewal and multilineage differentiation. Genes Dev. 2008; 22:1174–1189. [PubMed: 18451107]
12. Williams CJ, et al. The chromatin remodeler Mi-2beta is required for CD4 expression and T cell development. Immunity. 2004; 20:719–733. [PubMed: 15189737]
13. Gomez-Del Arco P, et al. The Chromatin Remodeling Complex Chd4/NuRD Controls Striated Muscle Identity and Metabolic Homeostasis. Cell Metab. 2016; 23:881–892. [PubMed: 27166947]
14. Kashiwagi M, Morgan BA, Georgopoulos K. The chromatin remodeler Mi-2beta is required for establishment of the basal epidermis and normal differentiation of its progeny. Development. 2007; 134:1571–1582. [PubMed: 17360773]
15. Werner S, Grose R. Regulation of wound healing by growth factors and cytokines. Physiol Rev. 2003; 83:835–870. [PubMed: 12843410]
16. Weaver CT, Hatton RD. Interplay between the TH17 and TReg cell lineages: a (co-)evolutionary perspective. Nat Rev Immunol. 2009; 9:883–889. [PubMed: 19935807]
17. Mohammed J, et al. TGFbeta1 overexpression by keratinocytes alters skin dendritic cell homeostasis and enhances contact hypersensitivity. J Invest Dermatol. 2013; 133:135–143. [PubMed: 22832490]
18. Yasmin N, et al. Identification of bone morphogenetic protein 7 (BMP7) as an instructive factor for human epidermal Langerhans cell differentiation. J Exp Med. 2013; 210:2597–2610. [PubMed: 24190429]
19. Strid J, Sobolev O, Zafirova B, Polic B, Hayday A. The intraepithelial T cell response to NKG2D-ligands links lymphoid stress surveillance to atopy. Science. 2011; 334:1293–1297. [PubMed: 22144628]
20. Willcox CR, et al. Cytomegalovirus and tumor stress surveillance by binding of a human gammadelta T cell antigen receptor to endothelial protein C receptor. Nat Immunol. 2012; 13:872–879. [PubMed: 22885985]
21. Witherden DA, et al. The CD100 receptor interacts with its plexin B2 ligand to regulate epidermal gammadelta T cell function. Immunity. 2012; 37:314–325. [PubMed: 22902232]
22. Stumptner-Cuvelette P, Benaroch P. Multiple roles of the invariant chain in MHC class II function. Biochim Biophys Acta. 2002; 1542:1–13. [PubMed: 11853874]

23. Deane JA, et al. Endogenous regulatory T cells adhere in inflamed dermal vessels via ICAM-1: association with regulation of effector leukocyte adhesion. J Immunol. 2012; 188:2179–2188. [PubMed: 22279104]
24. Kolls JK, McCray PB Jr, Chan YR. Cytokine-mediated regulation of antimicrobial proteins. Nat Rev Immunol. 2008; 8:829–835. [PubMed: 18949018]
25. Li M, et al. Retinoid X receptor ablation in adult mouse keratinocytes generates an atopic dermatitis triggered by thymic stromal lymphopoietin. Proc Natl Acad Sci U S A. 2005; 102:14795–14800. [PubMed: 16199515]
26. Li M, et al. Topical vitamin D3 and low-calcemic analogs induce thymic stromal lymphopoietin in mouse keratinocytes and trigger an atopic dermatitis. Proc Natl Acad Sci U S A. 2006; 103:11736–11741. [PubMed: 16880407]
27. Li J, et al. Counterregulation between thymic stromal lymphopoietin- and IL-23-driven immune axes shapes skin inflammation in mice with epidermal barrier defects. J Allergy Clin Immunol. 2016; 138:150–161. e113. [PubMed: 26993035]
28. He R, et al. TSLP acts on infiltrating effector T cells to drive allergic skin inflammation. Proc Natl Acad Sci U S A. 2008; 105:11875–11880. [PubMed: 18711124]
29. Demehri S, et al. Notch-deficient skin induces a lethal systemic B-lymphoproliferative disorder by secreting TSLP, a sentinel for epidermal integrity. PLoS Biol. 2008; 6:e123. [PubMed: 18507503]
30. Dumortier A, et al. Atopic dermatitis-like disease and associated lethal myeloproliferative disorder arise from loss of Notch signaling in the murine skin. PLoS One. 2010; 5:e9258. [PubMed: 20174635]
31. Lee HC, Ziegler SF. Inducible expression of the proallergic cytokine thymic stromal lymphopoietin in airway epithelial cells is controlled by NFkappaB. Proc Natl Acad Sci U S A. 2007; 104:914–919. [PubMed: 17213320]
32. Fontenot JD, Gavin MA, Rudensky AY. Foxp3 programs the development and function of CD4+CD25+ regulatory T cells. Nat Immunol. 2003; 4:330–336. [PubMed: 12612578]
33. Sakaguchi S, Yamaguchi T, Nomura T, Ono M. Regulatory T cells and immune tolerance. Cell. 2008; 133:775–787. [PubMed: 18510923]
34. Vignali DA, Collison LW, Workman CJ. How regulatory T cells work. Nat Rev Immunol. 2008; 8:523–532. [PubMed: 18566595]
35. Campbell DJ, Koch MA. Phenotypical and functional specialization of FOXP3+ regulatory T cells. Nat Rev Immunol. 2011; 11:119–130. [PubMed: 21267013]
36. Feuerer M, Hill JA, Mathis D, Benoist C. Foxp3+ regulatory T cells: differentiation, specification, subphenotypes. Nat Immunol. 2009; 10:689–695. [PubMed: 19536194]
37. Chen X, Baumel M, Mannel DN, Howard OM, Oppenheim JJ. Interaction of TNF with TNF receptor type 2 promotes expansion and function of mouse CD4+CD25+ T regulatory cells. J Immunol. 2007; 179:154–161. [PubMed: 17579033]
38. Setiady YY, Coccia JA, Park PU. In vivo depletion of CD4+FOXP3+ Treg cells by the PC61 anti-CD25 monoclonal antibody is mediated by FcgammaRIII+ phagocytes. Eur J Immunol. 2010; 40:780–786. [PubMed: 20039297]
39. Cretney E, et al. The transcription factors Blimp-1 and IRF4 jointly control the differentiation and function of effector regulatory T cells. Nat Immunol. 2011; 12:304–311. [PubMed: 21378976]
40. Quintana FJ, et al. Aiolos promotes TH17 differentiation by directly silencing Il2 expression. Nat Immunol. 2012; 13:770–777. [PubMed: 22751139]
41. Cretney E, Kallies A, Nutt SL. Differentiation and function of Foxp3(+) effector regulatory T cells. Trends Immunol. 2013; 34:74–80. [PubMed: 23219401]
42. Tomura M, et al. Activated regulatory T cells are the major T cell type emigrating from the skin during a cutaneous immune response in mice. J Clin Invest. 2010; 120:883–893. [PubMed: 20179354]
43. Dudda JC, Perdue N, Bachtanian E, Campbell DJ. Foxp3+ regulatory T cells maintain immune homeostasis in the skin. J Exp Med. 2008; 205:1559–1565. [PubMed: 18573908]
44. Shevach EM. Mechanisms of foxp3+ T regulatory cell-mediated suppression. Immunity. 2009; 30:636–645. [PubMed: 19464986]

45. Joller N, et al. Treg cells expressing the coinhibitory molecule TIGIT selectively inhibit proinflammatory Th1 and Th17 cell responses. Immunity. 2014; 40:569–581. [PubMed: 24745333]
46. Soumelis V, et al. Human epithelial cells trigger dendritic cell mediated allergic inflammation by producing TSLP. Nat Immunol. 2002; 3:673–680. [PubMed: 12055625]
47. Chinen T, et al. An essential role for the IL-2 receptor in Treg cell function. Nat Immunol. 2016
48. Rochman Y, et al. Thymic stromal lymphopoietin-mediated STAT5 phosphorylation via kinases JAK1 and JAK2 reveals a key difference from IL-7-induced signaling. Proc Natl Acad Sci U S A. 2010; 107:19455–19460. [PubMed: 20974963]
49. Bell BD, et al. The transcription factor STAT5 is critical in dendritic cells for the development of TH2 but not TH1 responses. Nat Immunol. 2013; 14:364–371. [PubMed: 23435120]
50. Isaksen DE, et al. Requirement for stat5 in thymic stromal lymphopoietin-mediated signal transduction. J Immunol. 1999; 163:5971–5977. [PubMed: 10570284]
51. Carpino N, et al. Absence of an essential role for thymic stromal lymphopoietin receptor in murine B-cell development. Mol Cell Biol. 2004; 24:2584–2592. [PubMed: 14993294]
52. Han H, Thelen TD, Comeau MR, Ziegler SF. Thymic stromal lymphopoietin-mediated epicutaneous inflammation promotes acute diarrhea and anaphylaxis. J Clin Invest. 2014; 124:5442–5452. [PubMed: 25365222]
53. Metzger D, Li M, Chambon P. Targeted somatic mutagenesis in the mouse epidermis. Methods Mol Biol. 2005; 289:329–340. [PubMed: 15502196]
54. Bettelli E, et al. Reciprocal developmental pathways for the generation of pathogenic effector TH17 and regulatory T cells. Nature. 2006; 441:235–238. [PubMed: 16648838]
55. Li H, Durbin R. Fast and accurate long-read alignment with Burrows-Wheeler transform. Bioinformatics. 2010; 26:589–595. [PubMed: 20080505]
56. Dobin A, et al. STAR: ultrafast universal RNA-seq aligner. Bioinformatics. 2013; 29:15–21. [PubMed: 23104886]
57. Anders S, Huber W. Differential expression analysis for sequence count data. Genome Biol. 2010; 11:R106. [PubMed: 20979621]
58. Love MI, Huber W, Anders S. Moderated estimation of fold change and dispersion for RNA-seq data with DESeq2. Genome Biol. 2014; 15:550. [PubMed: 25516281]
59. Huang da W, Sherman BT, Lempicki RA. Bioinformatics enrichment tools: paths toward the comprehensive functional analysis of large gene lists. Nucleic Acids Res. 2009; 37:1–13. [PubMed: 19033363]
60. Zhang J, et al. Harnessing of the nucleosome-remodeling-deacetylase complex controls lymphocyte development and prevents leukemogenesis. Nat Immunol. 2012; 13:86–94.

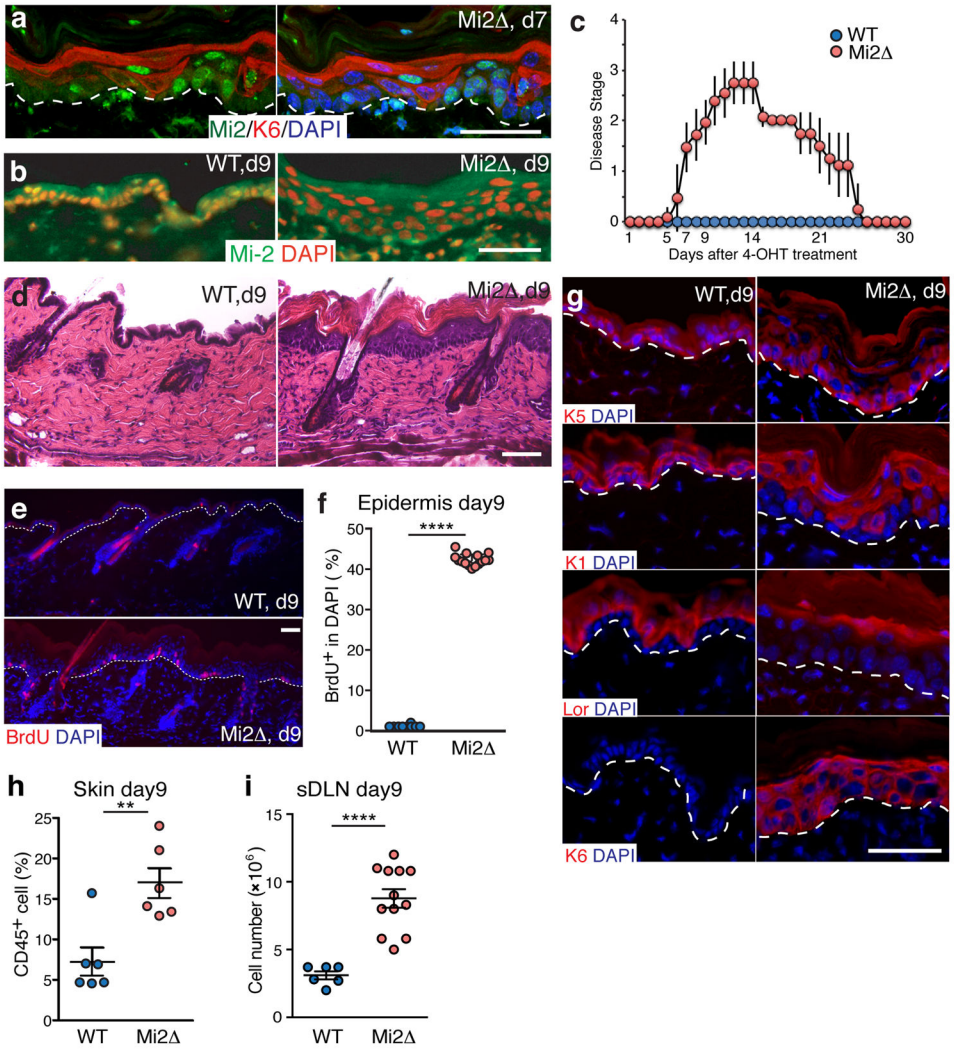

Figure 1. Loss of Mi-2β in the epidermis causes rapid keratinocyte activation

(**a** and **b**) Depletion of Mi-2β protein was evaluated by immunofluorescence at day 7 (**a**) or day 9 (**b**) after 4-OHT treatment. DAPI stained nuclei were shown in blue at day 7 and in red at day 9. At day 7, Keratin 6 (K6) expression (red) a marker of aberrant activation was confined to keratinocytes that lacked Mi-2β protein (green). At day 9, extensive depletion of Mi-2β was seen in Mi-2β mutant (Mi2Δ, red nuclear staining) compared to wild type (WT, yellow nuclei) epidermis. Scale bar, 50μm. (**c**) Time course of disease development and staging in Mi2Δ mice. 0, no clinical expression of disease; 1, rough hair coat on the ventral side; 1.5, rough hair coat on both sides; 2, loss of weight; 2.5, less movement; 3, hunched; 3.5, no movement, very thin; 4, dead. (**d**) Hematoxylin and Eosin-stained sections of wild-type and Mi2Δ skin. Scale bar, 50μm. (**e** and **f**) Proliferation of basal keratinocytes was measured by BrdU pulse-labeling. Skin sections with $BrdU^+$ cells (red) were shown in (**e**) with the dotted line demarcating the dermal-epidermal junction. The mean percent of $BrdU^+$ nuclei in the basal epidermis was shown in (**f**). Scale bar, 50μm. (**g**) Differentiation in the epidermis was assessed by expression of K5, K1 and Loricrin (Lor) and aberrant activation of K6 at day 9. DAPI stained nuclei were shown in blue and the dermal-epidermal junction

was demarcated with the dotted line. Scale bar, 50μm. (**h**) Percentage of $CD45^+$ leukocytes in the skin of wild-type and Mi2Δ, (**i**) Total cellularity of sDLNs of wild-type and Mi2Δ. $^{**}P < 0.01$ and $^{****}P < 0.0001$ (two-tailed unpaired t-test). Data shown are representative of three experiments with more than five Mi2Δ mice in (**a**), five experiments with more than ten mice per group in (**b, d** and **g**). Data shown in (**c**) were generated from ten experiments with WT N=20 and Mi2Δ N=32 mice analyzed at different time points (Day 7; WT N=5 Mi2Δ N=10, day 9; WT N=10 Mi2Δ N=12, day 14; WT N=2, Mi2Δ N N=4, day 21; WT N=2, Mi2Δ N=2, day 30; WT N=1, Mi2Δ N=4), in (**e** and **f**) from one experiment with WT N=10 and Mi2Δ N=15 independent sections from WT N=3 and Mi2Δ N=3 mice (mean+/− s.d.), in (**h**) from four independent experiments with WT N=6 and Mi2Δ N=6 mice (mean+/− s.e.m.), in (**i**) from six independent experiments with WT N=6 and Mi2Δ N=12 mice (mean+/− s.e.m.).

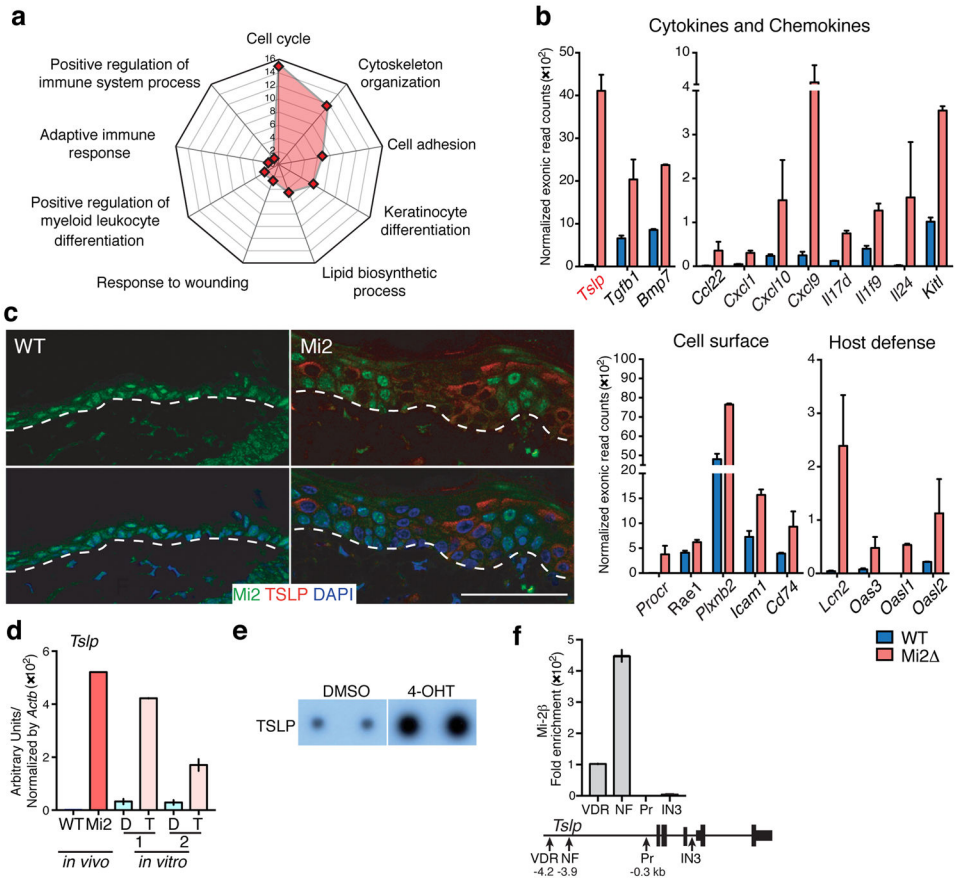

Figure 2. Mi-2β actively represses genes involved in keratinocyte activation and immune cell regulation

(**a**) Pathway analysis of genes that were significantly up-regulated in Mi2Δ keratinocytes relative to wild-type keratinocytes (up genes: 1201, *P* value < 0.05, > 2fold difference). Selected biological process GO terms and their associated *P* values ($-\log_{10}$) for pathway discovery are shown. (**b**) Expression of genes relevant to immune cell regulation shown as normalized exon mapping reads. (**c**) Early induction of TSLP expression (red) correlated with Mi-2β protein depletion in keratinocytes and was confined to cells that lacked Mi-2β (green). Scale bar, 50μm. (**d** and **e**) Mi-2β depletion in primary cultured keratinocytes resulted in induction of *Tslp* mRNA and protein secretion. (**d**) Induction of *Tslp* mRNA at 48h after *in vitro* induction of Mi-2β deletion. Sorted keratinocytes from *in vivo* wild-type and Mi-2β depleted epidermis were used as a control. D, DMSO, T, 4-OHT (**e**) Secretion of TSLP protein in the culture medium at 72h after induction of Mi-2β deletion. (**f**) Mi-2β ChIP-qPCR analysis of the TSLP locus in primary keratinocytes. VDR: Vitamin D3 response site, NF: NFκB response site, Pr: Promoter, IN3: Intron 3. Data were generated from two independent experimental groups with pooled samples from WT N=6 and Mi2Δ N=4 mice in (**a–b;** mean+/−s.e.m.). Data were representative of five independent experiments with ten mice per group in (**c**), two independent experiments with samples from Mi2Δ N=10 mice in (**d;** mean+/−s.e.m., each sample was tested in duplicate cultures in each experiment)**,** one experiment with pooled samples from Mi2Δ N=7 mice in (**e**), three

independent experiments in (**f;** mean+/−s.e.m., two independent PCR reactions in each experiment).

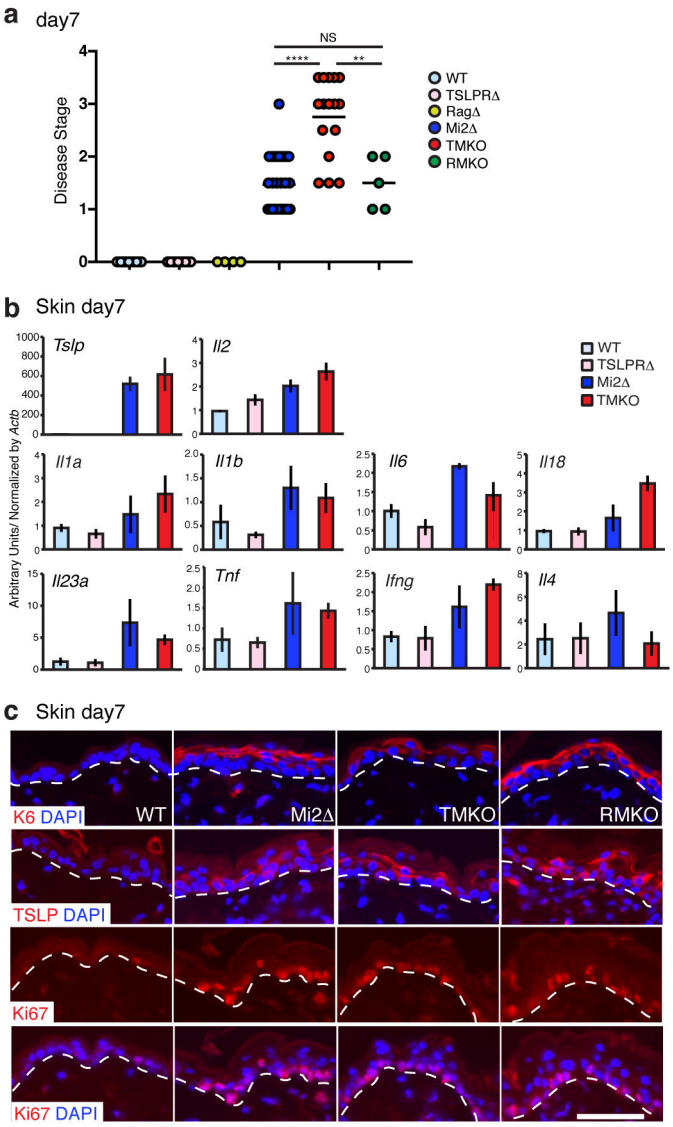

Figure 3. TSLPR protective role in skin pro-inflammatory responses

(**a**) Disease development and staging for 4-OHT treated mice at day 7 prior to becoming moribund. Each symbol in the graph indicated an individual mouse, and the group mean value was shown as a bar. $^{**}P < 0.01$, $^{****}P < 0.0001$, NS, not significant (two-tailed unpaired t-test). (**b**) Quantitative real-time PCR analysis of cytokine genes in skin biopsies from wild-type, TSLPRΔ, Mi2Δ and TMKO mice. (**c**) Expression of K6, the Ki67 antigen and TSLP was shown. DAPI stained nuclei were shown in blue. Scale bar, 50μm. Data were generated from WT N=30, TSLPRΔ N=16, RagΔ N=4, Mi2Δ N=32, TMKO N=16, and RMKO N=5 mice in (**a**). Data were representative of two independent experiments with at least three mice per group in (**b**; mean+/−s.d.), three independent experiments with more than five mice per group in (**c**).

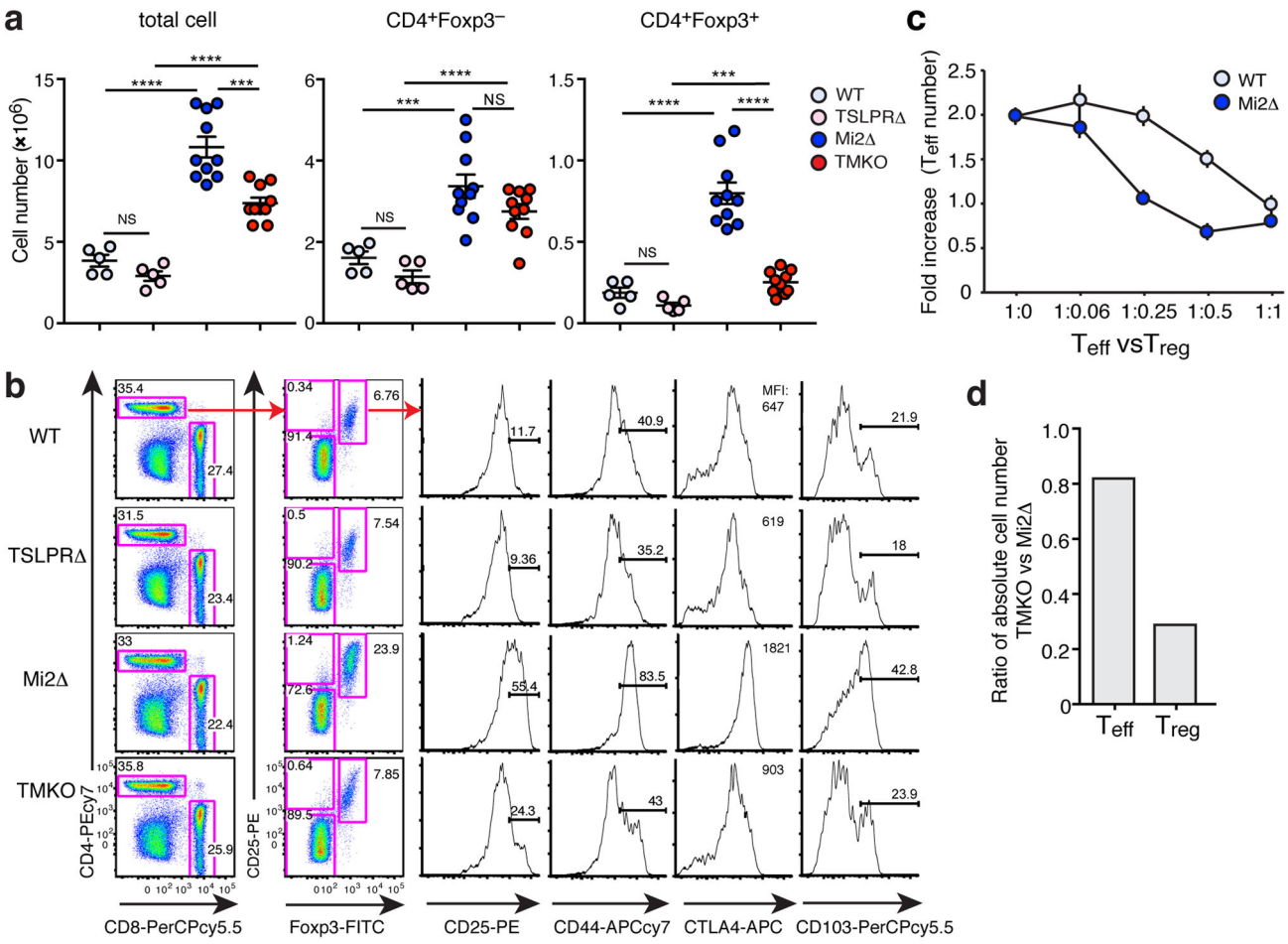

Figure 4. Activation of skin-associated T_{reg} cells is dependent on TSLPR signaling

(**a**) Total cellularity and absolute cell number of $CD4^+Foxp3^-$ and $CD4^+Foxp3^+$ in wild-type, TSLPRΔ, Mi2Δ and TMKO sDLNs were shown. ***$P < 0.001$, ****$P < 0.0001$, NS, not significant (two-tailed unpaired t-test). (**b**) Flow cytometric analysis of $CD4^+Foxp3^+$ T_{reg} cells, isolated from sDLNs of wild-type, TSLPRΔ, Mi2Δ, and TMKO mice, for activation and effector cell markers (CD25, CD44, CTLA4, CD103). (**c**) T_{reg} cells from sDLN of Mi2Δ mice were more potent suppressors of T_{eff} cell proliferation *in vitro* compared to wild-type counterparts. $CD4^+CD62L^+Foxp3\text{-}GFP^-$ T_{eff} cells were co-cultured with $CD4^+Foxp3\text{-}GFP^+$ T_{reg} cells from Mi2Δ sDLN at the indicated ratios (T_{eff}: T_{reg}) in the presence of irradiated APCs and anti-CD3ε for 3 days. T_{reg} cells from sDLNs or spleen of wild-type mice were used as controls. The T_{reg} effect on proliferation of T_{eff} cells was assessed by a change in cell number. (**d**) Ratio of absolute cell numbers for $CD4^+$ T cell subsets in TMKO vs. Mi2Δ sDLN was shown. Data shown in (**a** and **d**) were generated from five independent experiments with WT N=5, TSLPRΔ N=5, Mi2Δ N=10, and TMKO N=10 mice (mean+/− s.e.m.), in (**b**) were representative of four independent experiments with WT N=5, TSLPRΔ N=5, Mi2Δ N=4, TMKO, N=4 mice, and in (**c**) were representative of two independent experiments with pooled samples from wild-type N=14 Mi2Δ N=5 mice (mean +/− s.e.m.; each sample was tested in triplicate cultures in each experiment).

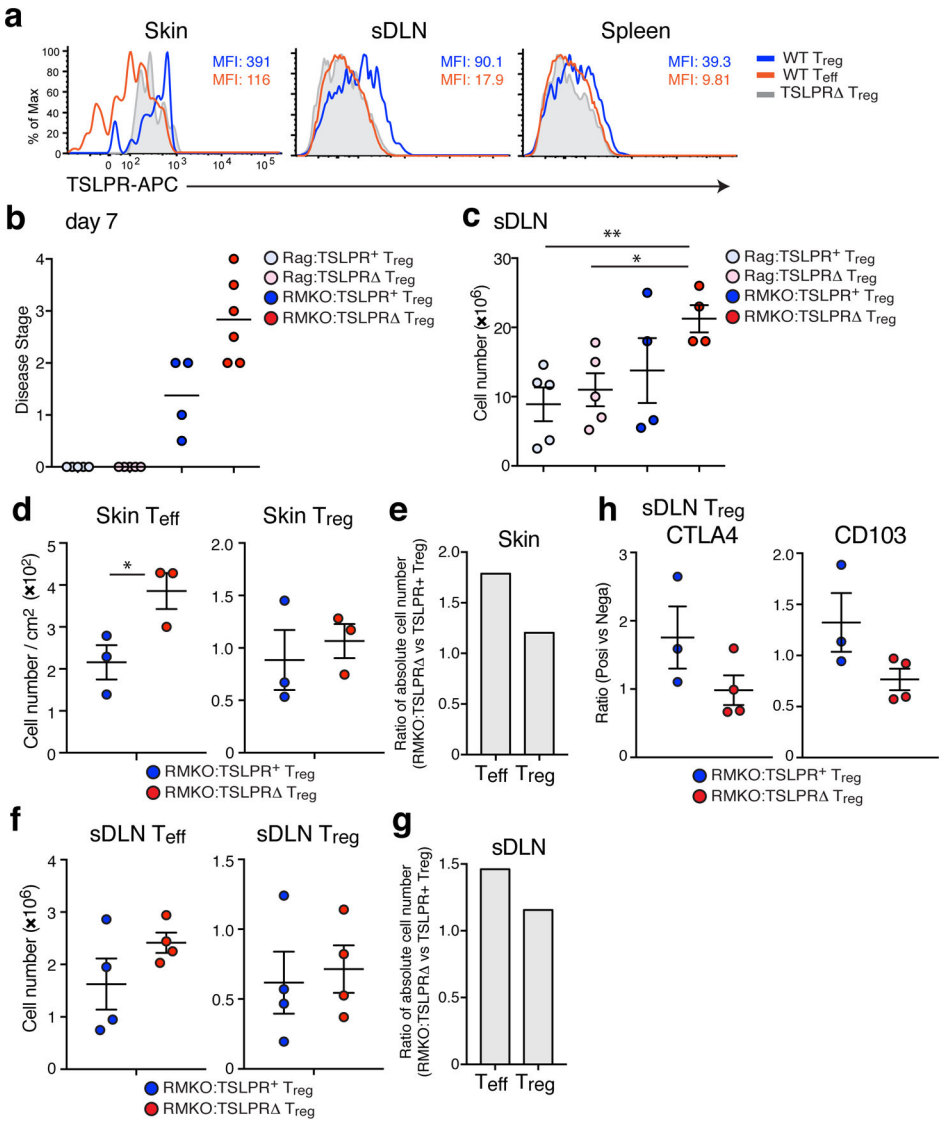

Figure 5. TSLPR signaling in T_{reg} cells supports immunosuppression and organismal homeostasis

(**a**) TSLPR expression is shown in $CD4^+Foxp3\text{-}GFP^+$ T_{reg} cells and $CD4^+Foxp3\text{-}GFP^-$ T_{eff} cells from skin, sDLN and spleen. (**b**) Disease development and staging for 4-OHT treated chimeric mice at day 7. Each symbol in the graph indicated an individual mouse and the group mean value is shown as a bar. (**c**) Total cellularity of sDLNs is shown. (**d–g**) TSLPRΔ T_{reg} cells were less potent at preventing expansion of T_{eff} cells compared to $TSLPR^+$ T_{reg} cells. Absolute cell numbers of T_{eff} and T_{reg} cells in the skin (**d**) and sDLNs (**f**) and their ratio in RMKO: TSLPRΔ T_{reg} vs. RMKO: $TSLPR^+$ T_{reg} chimeras in the skin (**e**) and sDLNs (**g**) are shown. (**h**) Ratio of positive vs. negative CTLA4 or CD103 subsets in RMKO: $TSLPR^+$ T_{reg} and RMKO: TSLPRΔ T_{reg} chimeras is shown. $*P < 0.05$, $**P < 0.01$ (two-tailed unpaired t-test). Data are representative of three independent experiments in (**a**), and generated from four independent experiments with Rag:$TSLPR^+T_{reg}$ N=5, Rag:$TSLPR\Delta T_{reg}$ N=5, RMKO:$TSLPR^+T_{reg}$ N=4, RMKO:$TSLPR\Delta T_{reg}$ N=6 in (**b–h;** mean+/−s.e.m.).

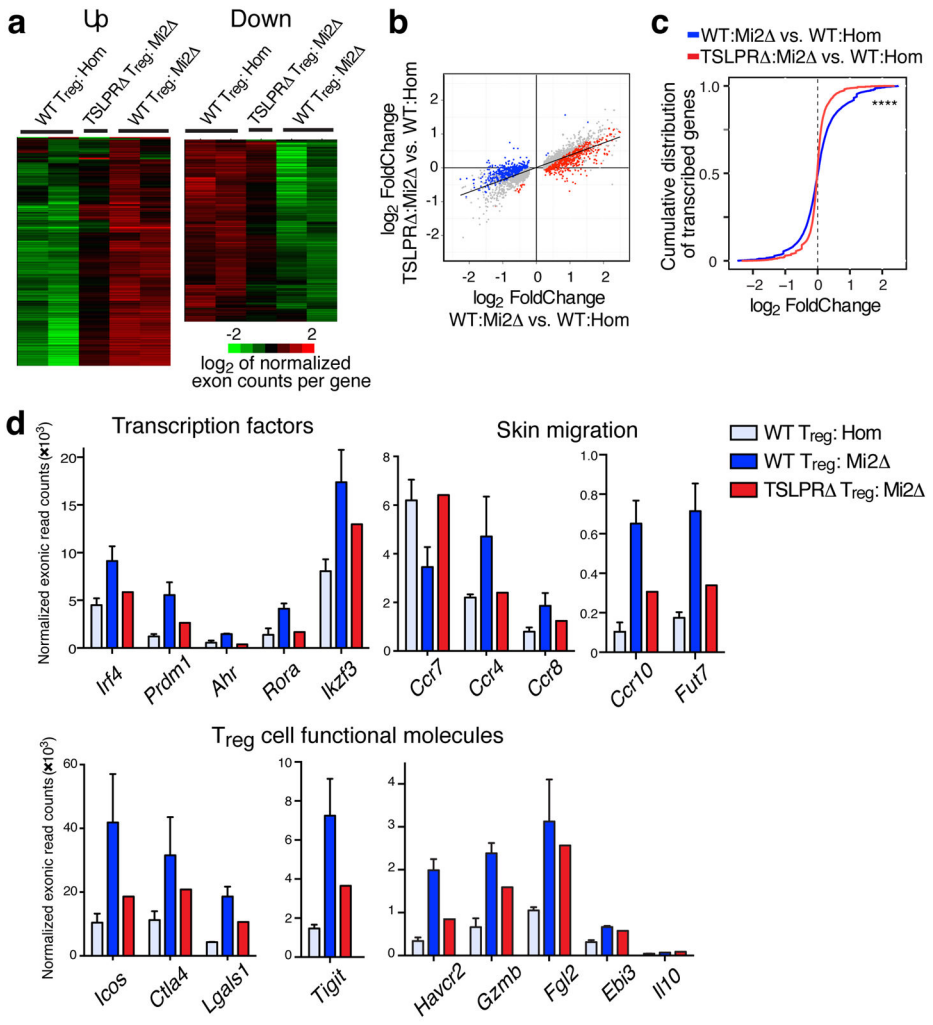

Figure 6. Transcriptional effects of TSLPR signaling in skin effector T_{reg} cells

(**a–c**) Transcriptional analysis of wild-type T_{reg}: Mi2Δ, TSLPRΔ T_{reg}: Mi2Δ, and wild-type T_{reg}: Hom cells. (**a**) Hierarchical clustering of differentially expressed genes in the three types of resting and activated T_{reg} cells is shown in a heatmap. (**b–c**) Differentially expressed genes in wild-type and TSLPRΔ T_{reg} cells from Mi-2β deficient pro-inflammatory skin compared to wild-type T_{reg} cells from homeostatic skin. Scatter plot of $\log_2$ fold changes (P <0.05) in gene expression is shown. Points that fall off the axis represent differentially expressed genes in T_{reg} cells under pro-inflammatory conditions that are dependent on TSLPR signaling. Genes that are up-regulated by >1.4 fold or down-regulated by >1.4 fold in wild-type T_{reg}: Mi2Δ compared to TSLPRΔ T_{reg}: Mi2Δ are highlighted in red and blue respectively. Unchanged genes are shown in gray. (**c**) Cumulative distribution function plot depicting a highly significant change in gene expression between wild-type and TSLPRΔ T® cells from Mi-2β deficient skin. ****P < 0.0001 was calculated by the Kolmogorov-Smirnov test, (**d**) Differentially expressed genes (mean+/−s.e.m.) encoding transcription factors, chemokine receptors and other molecules implicated in T_{reg} cell function is shown for the three types of T_{reg} cells. Data shown were generated from two

independent experimental groups with pooled T_{reg} cells from sDLN of WT N=7, Mi2Δ N=2, and TMKO N=6 mice in each.